Bi-directional and shared epigenomic signatures following proton and ^{56}Fe irradiation

Running title: Proton irradiation, cognition, DNA methylation, and gene expression

Soren Impey [a, b #], Timothy Jopson [c], Carl Pelz [a], Amanuel Tafessu [a], Fatema Fareh [a], Damian Zuloaga [d], Tessa Marzulla [d], Lara-Kirstie Riparip [c], Blair Stewart [d], Susanna Rosi [c], Mitchell S. Turker [e], and Jacob Raber [d, f #]

[a] Oregon Stem Cell Center and Department of Pediatrics, Oregon Health and Science University, Portland, OR 97239 USA

[b] Department of Cell and Developmental Biology, Oregon Health and Science University, Portland, OR 97239 USA

[c] Brain and Spinal Injury Center, Departments of Neurological Surgery and Physical Therapy and Rehabilitation Science, University of California, San Francisco, San Francisco, CA, 94110 USA

[d] Department of Behavioral Neuroscience, Oregon Health and Science University, Portland, OR 97239 USA

[e] Oregon Institute of Occupational Health Sciences and Department of Molecular and Medical Genetics, Oregon Health and Science University, Portland, OR 97239

[f] Departments of Neurology and Radiation Medicine, Division of Neuroscience ONPRC, Oregon Health and Science University, Portland, OR 97239, USA

Proton 2w 0 Gy

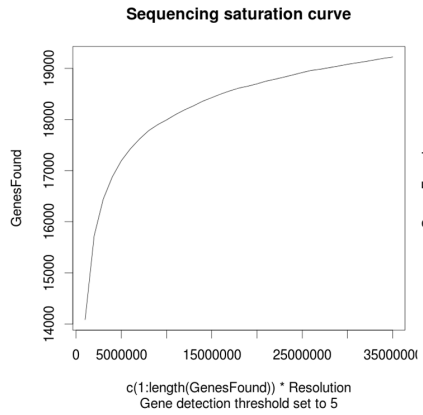

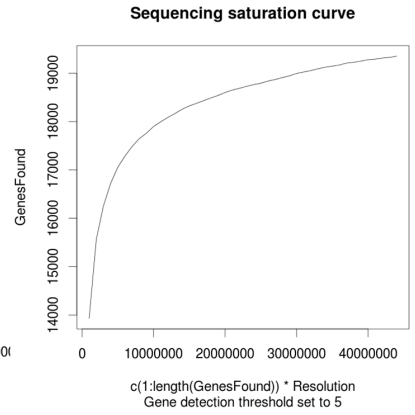

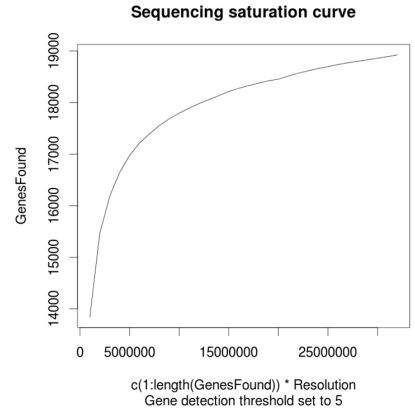

Proton 2w 1 Gy

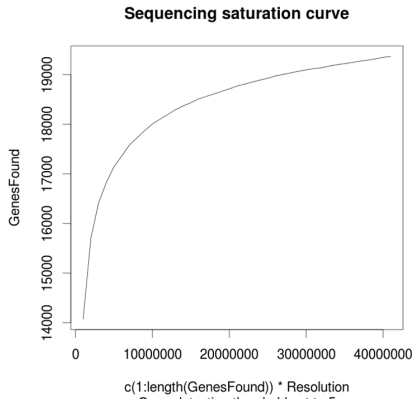

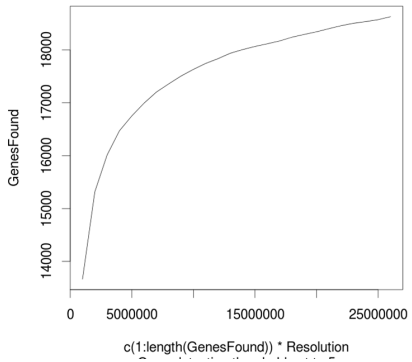

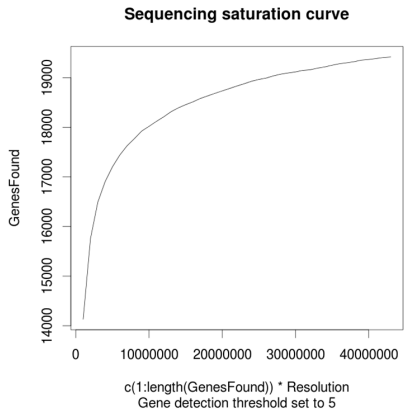

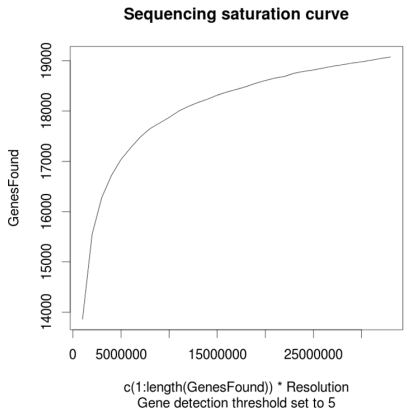

Suppl Fig 1

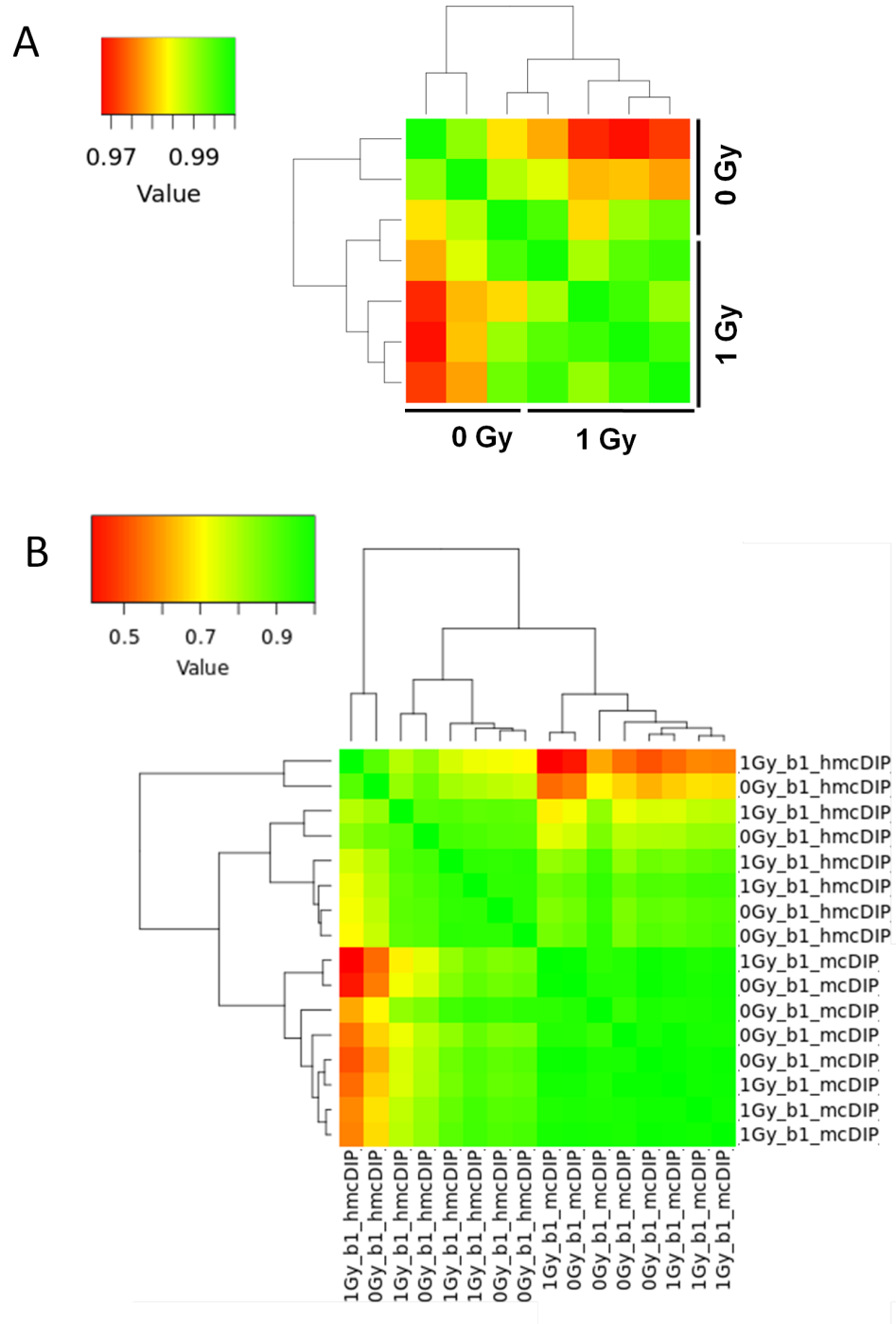
A
0.97
0.99
Value
0 Gy
1 Gy
0 Gy
1 Gy
B
0.5
0.7
0.9
Value
1Gy_b1_hmcDIP
0Gy_b1_hmcDIP
1Gy_b1_hmcDIP
0Gy_b1_hmcDIP
1Gy_b1_hmcDIP
1Gy_b1_hmcDIP
0Gy_b1_hmcDIP
0Gy_b1_hmcDIP
1Gy_b1_mcDIP
0Gy_b1_mcDIP
0Gy_b1_mcDIP
0Gy_b1_mcDIP
0Gy_b1_mcDIP
1Gy_b1_mcDIP
1Gy_b1_mcDIP
1Gy_b1_mcDIP
1Gy_b1_hmcDIP
0Gy_b1_hmcDIP
1Gy_b1_hmcDIP
0Gy_b1_hmcDIP
1Gy_b1_hmcDIP
1Gy_b1_hmcDIP
0Gy_b1_hmcDIP
0Gy_b1_hmcDIP
1Gy_b1_mcDIP
0Gy_b1_mcDIP
0Gy_b1_mcDIP
0Gy_b1_mcDIP
0Gy_b1_mcDIP
1Gy_b1_mcDIP
1Gy_b1_mcDIP
1Gy_b1_mcDIP

Suppl Fig 2

Scatter Plot 5mC vs 5hmC

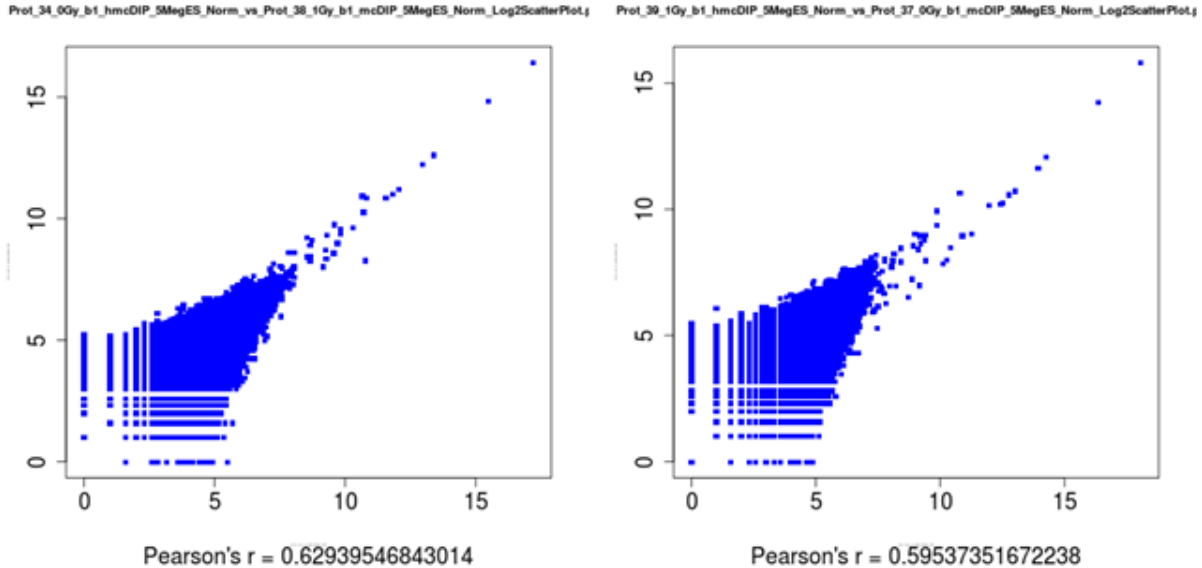

Scatter Plot 5hmC vs 5hmC

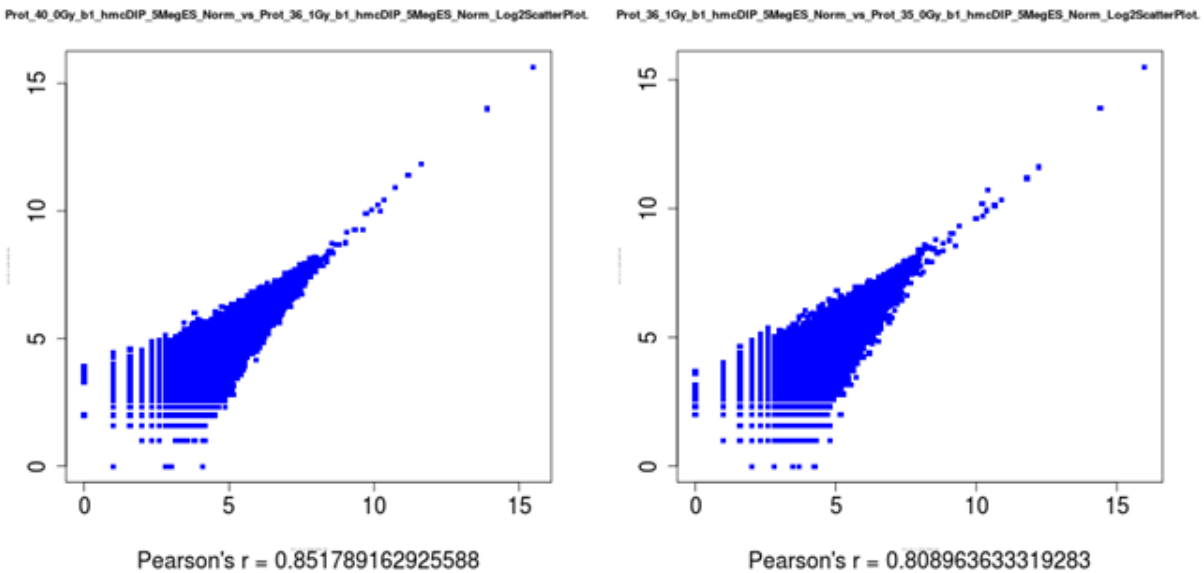

Suppl Fig 3

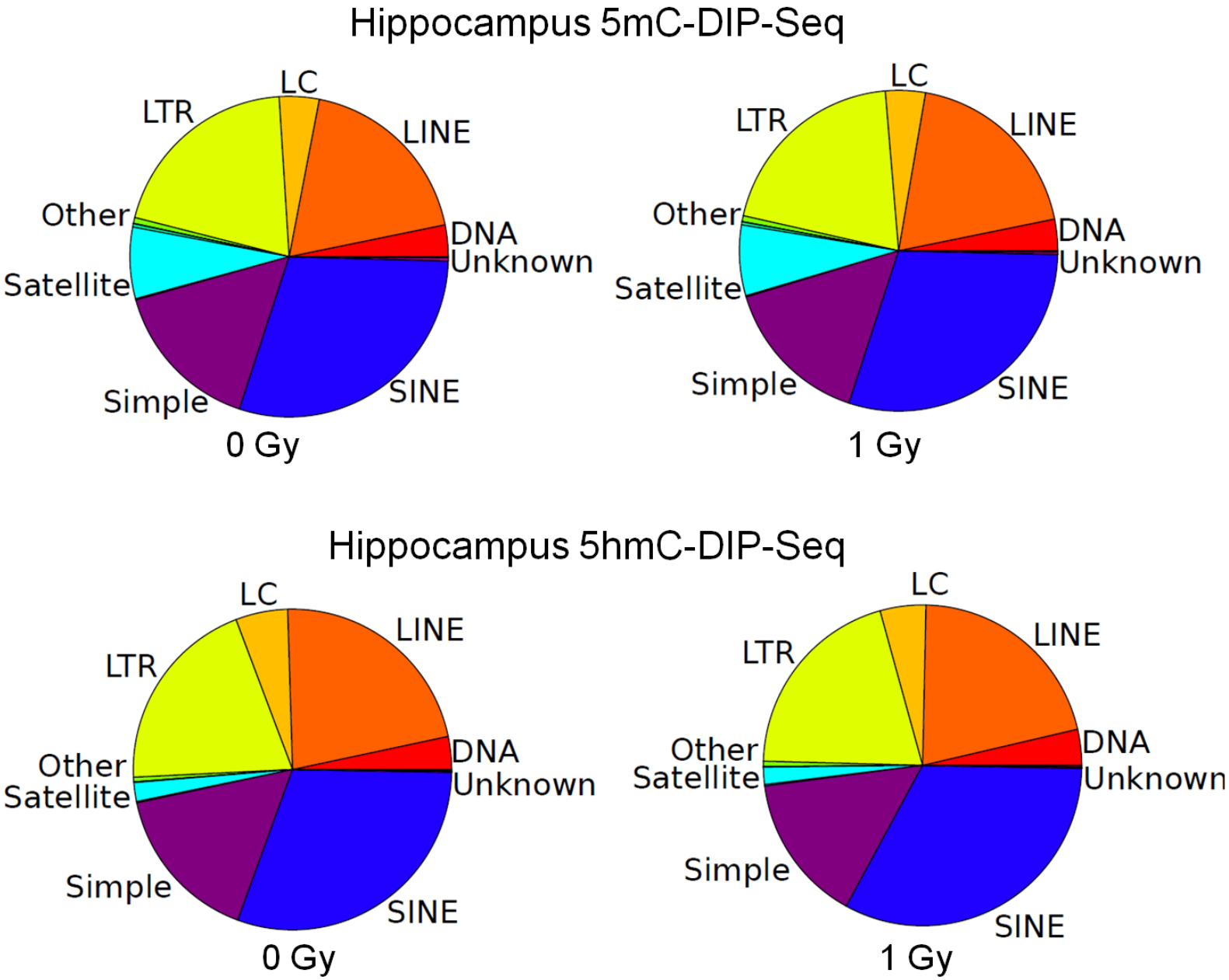
Hippocampus 5mC-DIP-Seq
LC
LTR
LINE
Other
DNA
Unknown
Satellite
Simple
SINE
0 Gy
LC
LTR
LINE
Other
DNA
Unknown
Satellite
Simple
SINE
1 Gy
Hippocampus 5hmC-DIP-Seq
LC
LTR
LINE
Other
DNA
Unknown
Satellite
Simple
SINE
0 Gy
LC
LTR
LINE
Other
DNA
Unknown
Satellite
Simple
SINE
1 Gy

Suppl Fig 4

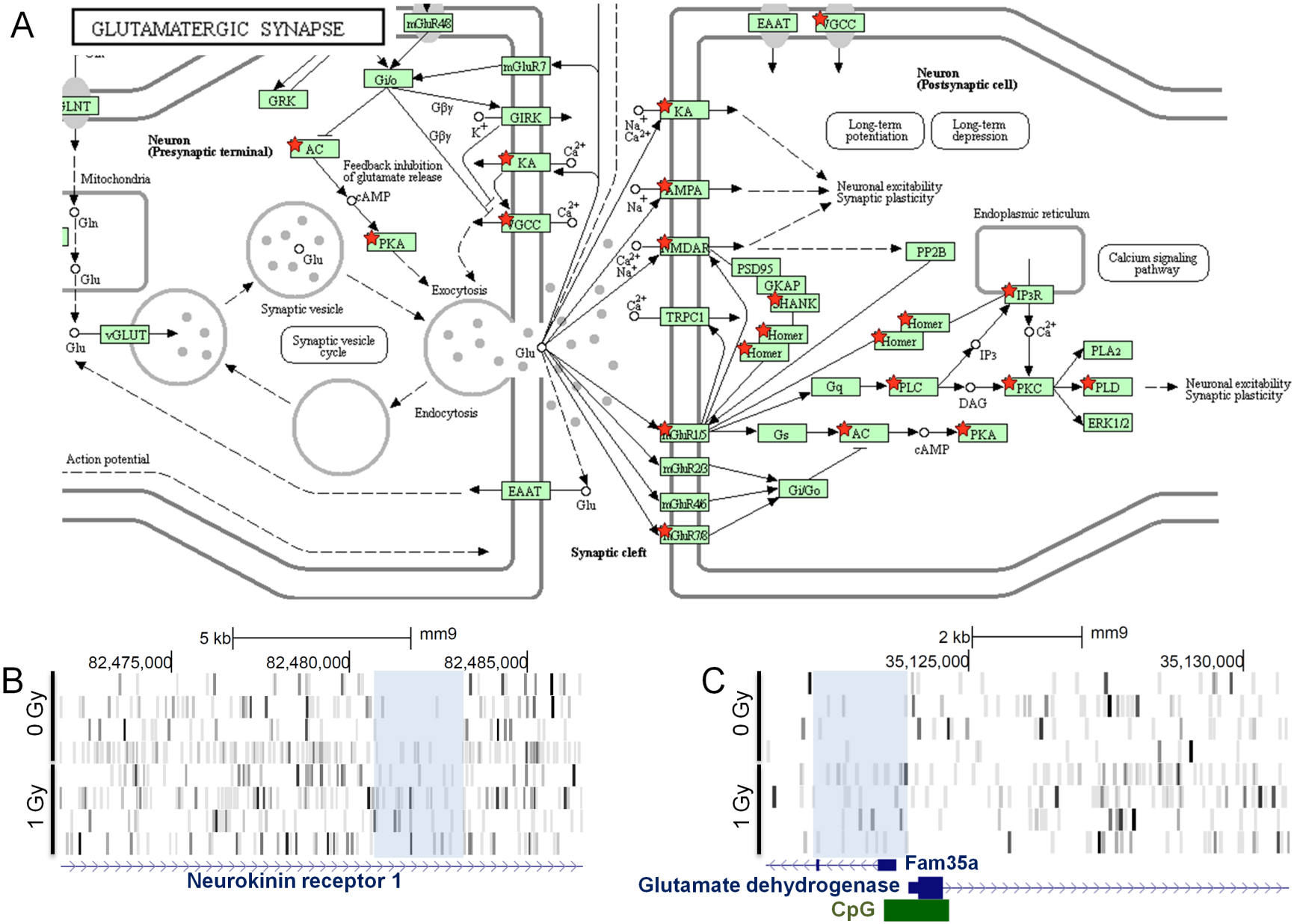
A
GLUTAMATERGIC SYNAPSE
Neuron
(Presynaptic terminal)
Neuron
(Postsynaptic cell)
Synaptic cleft
Mitochondria
Synaptic vesicle
Synaptic vesicle cycle
Exocytosis
Endocytosis
Action potential
Feedback inhibition of glutamate release
cAMP
Long-term potentiation
Long-term depression
Neuronal excitability
Synaptic plasticity
Endoplasmic reticulum
Calcium signaling pathway
DAG
IP3
cAMP
Gln
Glu
vGLUT
GRK
AC
PKA
VGCC
GIRK
KA
AMPA
NMDAR
TRPC1
PSD95
GKAP
SHANK
Homer
PP2B
IP3R
PLC
PKC
PLA2
PLD
ERK1/2
Gq
Gs
Gi/Go
EAAT
mGluR1/5
mGluR2/3
mGluR4/6
mGluR7/8
B
5 kb
mm9
82,475,000
82,480,000
82,485,000
0 Gy
1 Gy
Neurokinin receptor 1
C
2 kb
mm9
35,125,000
35,130,000
0 Gy
1 Gy
Fam35a
Glutamate dehydrogenase
CpG

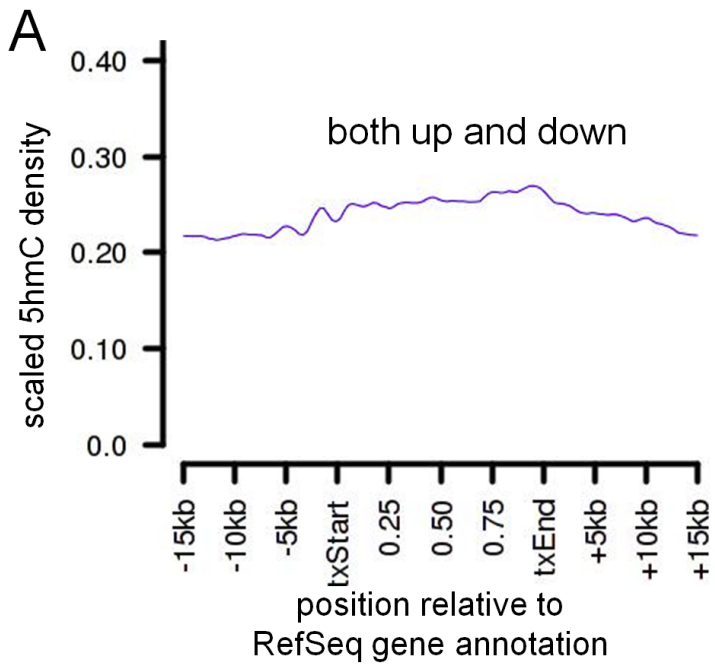
A
both up and down
scaled 5hmC density
0.40
0.30
0.20
0.10
0.0
-15kb
-10kb
-5kb
txStart
0.25
0.50
0.75
txEnd
+5kb
+10kb
+15kb
position relative to
RefSeq gene annotation

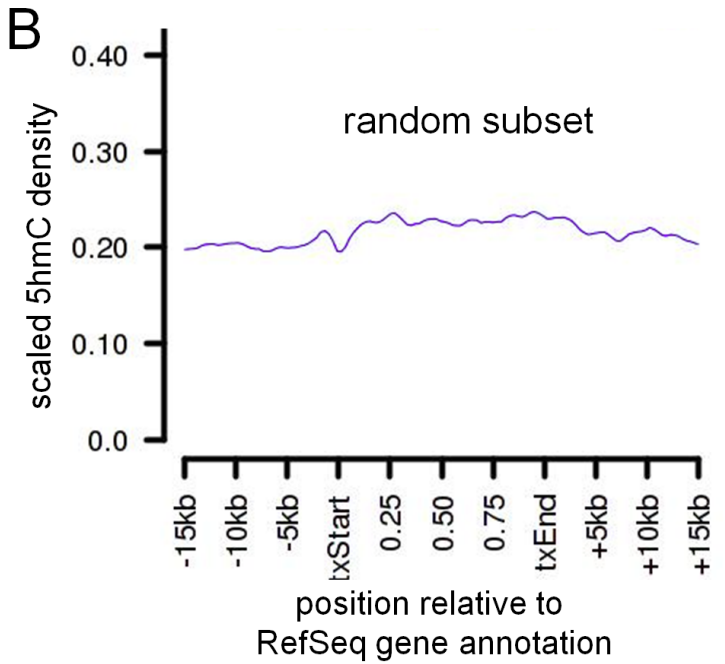
B
random subset
scaled 5hmC density
0.40
0.30
0.20
0.10
0.0
-15kb
-10kb
-5kb
txStart
0.25
0.50
0.75
txEnd
+5kb
+10kb
+15kb
position relative to
RefSeq gene annotation

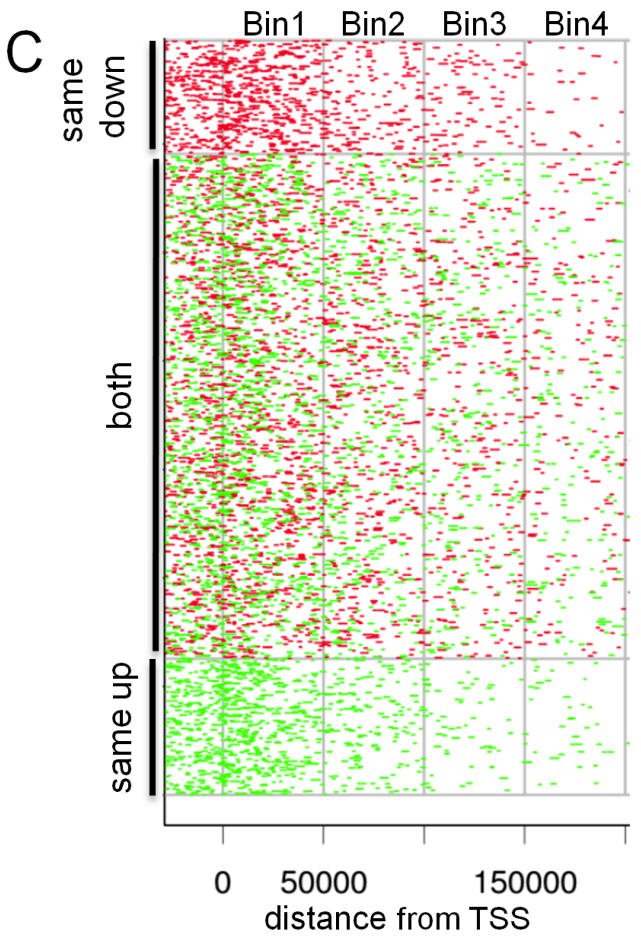
C
Bin1
Bin2
Bin3
Bin4
same down
both
same up
0
50000
150000
distance from TSS

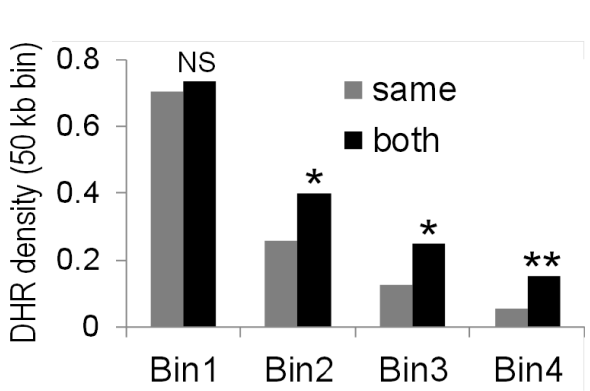
D
DHR density (50 kb bin)
0.8
0.6
0.4
0.2
0
NS
*
*
**
same
both
Bin1
Bin2
Bin3
Bin4

Suppl Fig 6

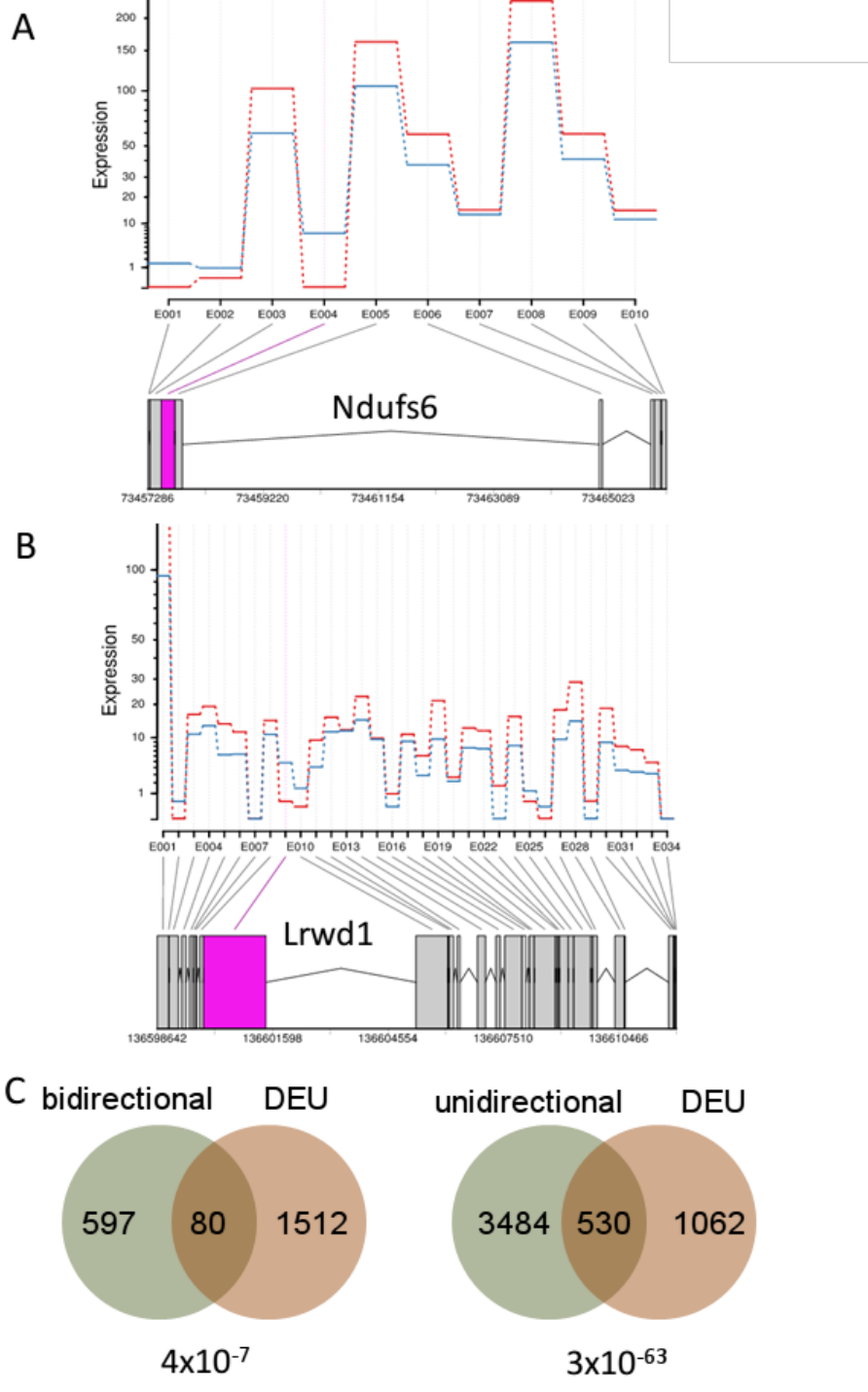
A
Expression
200
150
100
50
30
20
10
1
E001 E002 E003 E004 E005 E006 E007 E008 E009 E010
Ndufs6
73457286 73459220 73461154 73463089 73465023
B
Expression
100
50
30
20
10
1
E001 E004 E007 E010 E013 E016 E019 E022 E025 E028 E031 E034
Lrwd1
136598642 136601598 136604554 136607510 136610466
C
bidirectional
DEU
597
80
1512
4x10-7
unidirectional
DEU
3484
530
1062
3x10-63

Suppl Fig 7

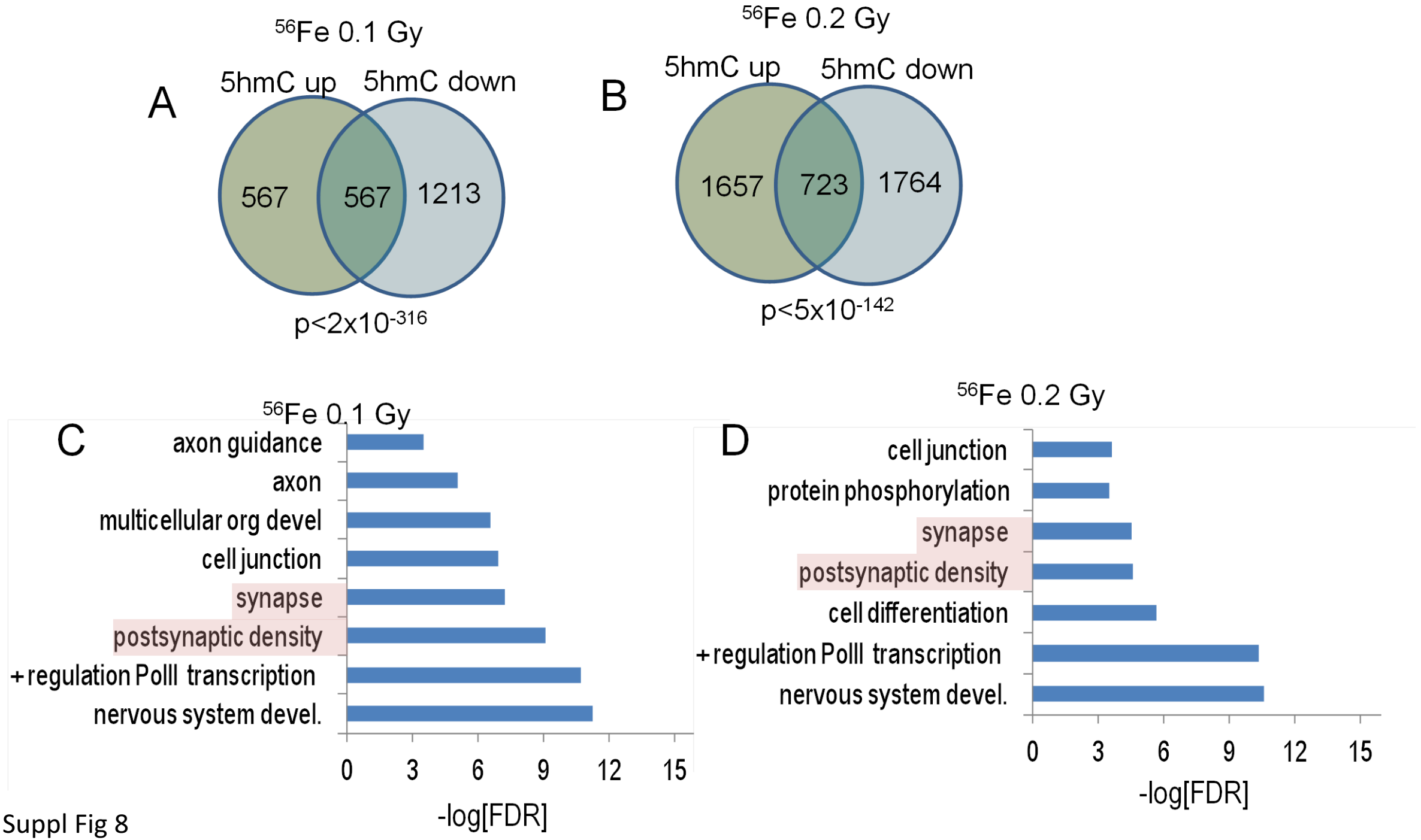
A
^{56}Fe 0.1 Gy
5hmC up
5hmC down
567
567
1213
p<2x10^{-316}
B
^{56}Fe 0.2 Gy
5hmC up
5hmC down
1657
723
1764
p<5x10^{-142}
C
^{56}Fe 0.1 Gy
axon guidance
axon
multicellular org devel
cell junction
synapse
postsynaptic density
+regulation PolII transcription
nervous system devel.
0
3
6
9
12
15
-log[FDR]
D
^{56}Fe 0.2 Gy
cell junction
protein phosphorylation
synapse
postsynaptic density
cell differentiation
+regulation PolII transcription
nervous system devel.
0
3
6
9
12
15
-log[FDR]

Suppl Fig 8

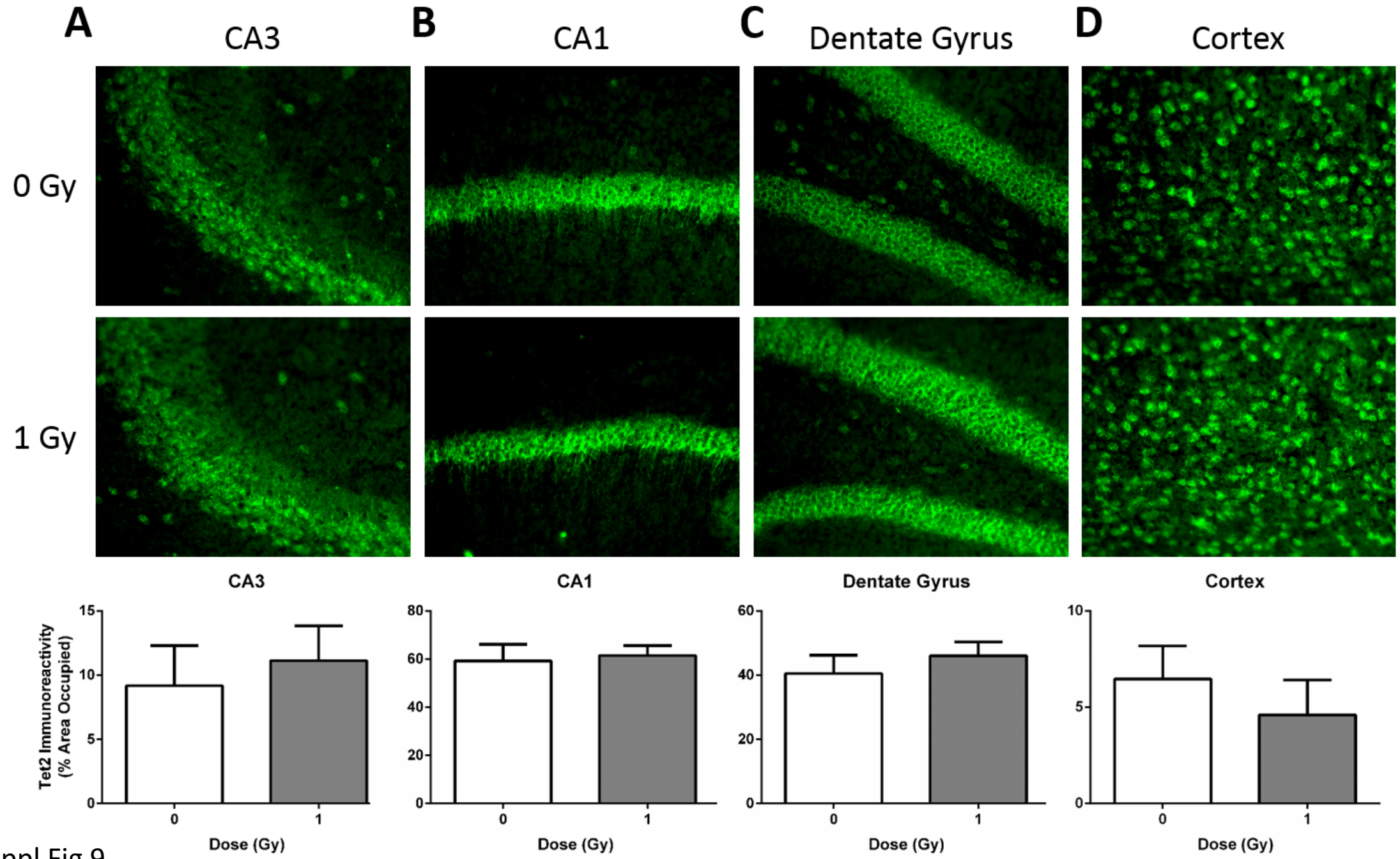
A
CA3
B
CA1
C
Dentate Gyrus
D
Cortex
0 Gy
1 Gy
CA3
CA1
Dentate Gyrus
Cortex
Tet2 Immunoreactivity (% Area Occupied)
Dose (Gy)
Dose (Gy)
Dose (Gy)
Dose (Gy)

Suppl Fig 9

Suppl. Figure Legends

Suppl. Fig. 1. R**NA-**Seq saturation curves at depth of 5 reads per annotated gene.

Suppl. Fig. 2. (A) Pearson correlation matrix of log2-transformed RNA-Seq exonic reads. The color scale shows Pearson's *r*. (B) Pearson correlation matrix of 5mC- and 5hmC-DIP-Seq reads from indicated samples. Reads were selected from regions of enrichment (FDR-adjusted $p < 0.001$) merged across all samples.

Suppl. Fig. 3. Example correlation scatter plots for some of the comparisons in Suppl. Fig. 2B.

Suppl. Fig. 4. Both 5mc and 5hmC regions are enriched at major parasitic repeats (LINEs, SINEs, LTR-based repeated) with 5mC showing the expected enrichment at Satellite repeats.

Suppl. Fig. 5. KEGG analyses revealed that synapse pathways are significantly associated with increased DHRs. The KEGG database was developed by the Kanehissa Laboratories, as described [72].

Suppl. Fig. 6. A and B. Similar global 5hmC density levels at genes with overlapping up and down DHRs versus a random subset of up alone or down alone. C. Heatmap shows up (green)

and down (red) DHRs from a subset of genes that are >200 kb in genomic length, have two up (same up), two down (same down), or an up and down (both) DHR, and are then randomly sorted by the directionality of intragenic DHRs (horizontal grey line). The indicated bins (grey lines) delineate 50 kb regions distal to the transcriptional start site (TSS). D. A permutation statistic identifies a highly significant increase in DHR density in distal bins for genes with "both" versus genes with "same" DHR distributions (see C). *$p < 1x10^{-4}$ and **$p < 2x10^{-7}$.

Suppl. Fig. 7. Differential exon usage anlaysis. A and B. Gene ideograms depict significantly regulated genes with exon expression levels for 0 Gy and 1 Gy indicated by the red and blue lines respectively. The significantly-regulated exon is highlighted. C. Venn diagram depicts intersection of 677 bidirectional DHRs and 4014 unidirectional DHRs with annotated differentially-expressed exons ($p < 0.01$). The fisher exact test was used to assess significance.

Suppl. Fig. 8. Reanalyzing the ^{56}Fe data using a similar bioinformatics pipeline as used in the current study, we once again observed a strikingly significant overlap between increased and decreased DHRs at the same genes for both the 0.1 Gy and 0.2 Gy doses.

Suppl. Fig. 9. Comparable Tet2 immunoreactivity in sham-irradiated and proton irradiated mice at the 2-week time point. **A.** Tet2 immunoreactivity levels in the CA3 region of the hippocampus. *$p < 0.05$ versus sham-irradiation. **B.** Tet2 immunoreactivity levels in the CA1

region of the hippocampus. **C.** Tet2 immunoreactivity levels in the dentate gyrus. **D.** Tet2 immunoreactivity levels in the cortex. $N = 20$ mice/dose.